Effects of Doping in the Active Region of 630-nm Band GaInP–AlGaInP Tensile-Strained Quantum-Well Lasers

Shun Tung Yen and Chien-Ping Lee, *Senior Member, IEEE*

***Abstract*— We theoretically analyze 630-nm band GaInP-AlGaInP tensile-strained quantum-well (QW) lasers with doping in the active region. The radiative current can be significantly reduced by introducing n-type doping in the active region. However, this advantage is reduced by the increase of the leakage current. As a result, the threshold current is reduced and the emission wavelength is shortened for multiquantum-well (MQW) lasers by n-type doping. But for single-quantum-well (SQW) lasers, because of the large increase of the leakage current, the threshold current increases with n-type doping.**

***Index Terms*— Doped lasers, quantum well, quantum-well lasers, semiconductor device modeling, semiconductor lasers, spontaneous emission, visible lasers.**

I. Introduction

RECENTLY, there have been extensive studies on short-wavelength GaInP–AlGaInP strained quantum-well (QW) lasers for their applications to optical data storage, laser printers, bar-code readers, etc. The threshold current of such lasers is typically high due to the inherent limitation of the laser material system. This problem is serious especially for lasers emitting at the 630-nm band. The threshold current can be reduced by introducing tensile or compressive strain to QW's [1]–[5]. However, the reduction of the threshold current is limited because the leakage current which plays an important part of the threshold current can not be suppressed effectively. A great reduction of the threshold current has been demonstrated by n-type doping in the active region of lasers in (In)GaAs–AlGaAs and InGaAsP–InP systems [6]–[9]. In addition, the n-type doped lasers have a shorter emission wavelength compared with that of undoped lasers [7]. A short emission wavelength is desired for application in optical data storage. The mechanism of the threshold current in 630-nm GaInP–AlGaInP lasers is more complicated than that of these lasers which have a negligible leakage current. Introducing doping to the active region of GaInP–AlGaInP lasers may affect not only the radiative current and the emission wavelength but also the leakage current.

In this paper, the effects of doping in the active region of 630-nm band GaInP–AlGaInP lasers are investigated theoretically. The calculation method is described briefly in Section II. The results indicate that both the threshold current and the emission wavelength can be improved by introducing n-type doping in the active region of multiquantum-well (MQW) lasers. However, there is no advantage of reducing the threshold current by introducing n-type doping for single-quantum-well (SQW) lasers.

Manuscript received August 22, 1997; revisec October 23, 1997. This work was supported by the National Science Council of the Republic of China under Contract NSC84-2215-E009-039.

The authors are with the Department of Electronics Engineering, National Chiao Tung University, Hsinchu, Taiwan, R.O.C.

Publisher Item Identifier S 0018-9197(98)06238-1.

II. Calculation Method

The major part of the calculation method used in this paper has been described in detail in our previous work [10]. We consider lasers with a conventional step-index separate confinement heterostructure (SCH). Shown in Fig. 1 is the illustration for the band profile around the active region of the lasers at threshold. The band profile is assumed to be nearly flat in this situation. There are two types of states taken into account in the calculation. One is the bound states confined to the QW's. The other is the continuum states lying in the subbands with energy higher than the barrier. The subbands are continuum because one side of the conduction and the valence band profiles is open. In practical calculation, the continuum states are discretized by imposing a fictitious infinite potential barrier far away from the active region on the open side [10]. We consider the distribution of carriers in the two types of states and the transitions between these states. The total optical transition is therefore composed of four components: 1) the bound-to-bound ($b \rightarrow b$); 2) the bound-to-continuum ($b \rightarrow c$); 3) the continuum-to-bound ($c \rightarrow b$); and 4) the continuum-to-continuum ($c \rightarrow c$) transitions. The continuum states are generally neglected in theoretical analysis of QW lasers. It has, however, been demonstrated that for 630-nm band GaInP–AlGaInP lasers, a large amount of carriers may spill over the barriers from the wells and hence the optical transitions involving the continuum states are of considerable importance [10]. They result in a significant contribution to the optical gain (or loss) and the radiative recombination current.

The bound valence states are obtained by using the 6×6 Luttinger–Kohn Hamiltonian which contains the deformation potentials to consider the strain effect [11]. The inclusion of the coupling of the spin-orbital split-off bands to the Hamiltonian is necessary for such short-wavelength lasers since the split-off energy of the wide bandgap material is small (~0.1 eV). In calculating the continuum states, we do not consider the band mixing and assume that the active region is bound within

0018–9197/98$10.00 © 1998 IEEE

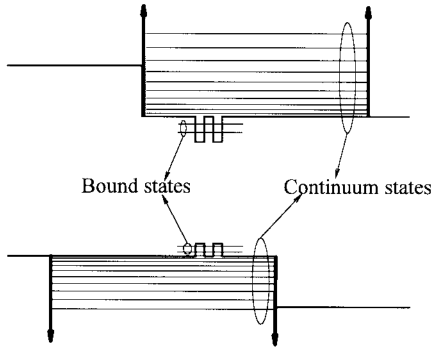

Fig. 1. The illustration for band profile at threshold.

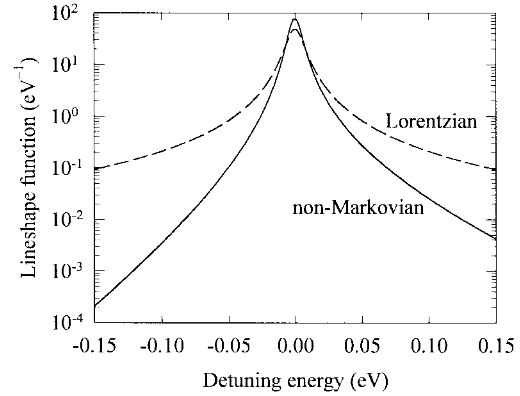

Fig. 2. The non-Markovian lineshape function (solid line) with $C = 0.005$ eV, $K_1 = 10$ eV^{-1}, and $K_2 = 30$ eV^{-1} and the Lorentzian lineshape function (dashed line) with a 0.1-ps relaxation lifetime.

two infinite potential barriers separated far enough away (see Fig. 1) [12]. We obtain the bound conduction states and the continuum states (for both the conduction band and the valence band) by solving the one-band effective mass equation [10]. Once the wave functions and their energies are solved, the momentum matrix elements, all components of the gain, and those of the spontaneous emission rate can be obtained using the formulas in [10].

The threshold condition is written as

$$\Gamma_{QW}(g_{b\to b} + g_{b\to c} + g_{c\to b}) + \Gamma_{WG} g_{c\to c} = \alpha_i + \alpha_m \quad (1)$$

where $g_{b\to b}, g_{b\to c}, g_{c\to b}$, and $g_{c\to c}$ are the gain coefficients arising from the four different transitions. α_i is the internal loss due to other loss mechanisms and α_m is the mirror loss. Γ_{QW} is the optical confinement factor for the QW region. (For MQW lasers, the QW region is defined to be composed of the QW's and the barriers sandwiched by the wells.) Γ_{WG} is the confinement factor for the waveguide region which is defined here to be composed of the confining layers and the QW region. In calculating the threshold condition, the quasi-equilibrium is assumed. One can therefore find the quasi-Fermi levels at threshold for the conduction and the valence bands by (1). Once the threshold condition is found, one can further calculate the four components of the spontaneous emission rates at threshold. The radiative recombination currents are obtained using [10, eqs. (32), (33)].

It is worth emphasizing that the lineshape broadening resulting from the carrier intraband relaxation is important in determining the gain spectrum. A simple Lorentzian lineshape function is usually used in the gain calculation. It is, however, improper for gain calculation in this work. The slow lineshape tail of the Lorentzian lineshape on the low-energy side gives rise to an unreasonably large absorption of photons with energy well below the bandgap, inconsistent with the observed result. In this study, the choice of the lineshape function is especially important since the continuum states are included in the calculation. A poorly chosen lineshape will result in a large absorption loss due to the optical transition between the continuum states. The actual lineshape function should be derived by considering the non-Markovian relaxation processes in the QW [13], [14]. However, deriving the non-Markovian lineshape from the first principle will greatly increase the complication and the computation time in device simulation. It is found that the non-Markovian lineshape can be well fitted by the simple form

$$L(E) = \frac{1}{N}\,\frac{\Gamma(E)}{E^2 + \Gamma^2(E)} \quad (2)$$

with

$$\Gamma(E) = Ce^{K_1 E}E^{-K_2|E|} \quad (3)$$

where N is chosen so that the lineshape function $L(E)$ is normalized and C, K_1, and K_2 are fitting parameters. In the gain calculation, we use the non-Markovian lineshape plotted in Fig. 2 with $C = 0.005$ eV, $K_1 = 10$ eV^{-1}, and $K_2 = 30$ eV^{-1}. Also shown in the figure is the conventional Lorentzian lineshape with a 0.1-ps relaxation lifetime. Obviously, the non-Markovian lineshape has a much steeper tail on the low-energy side.

The dopants are assumed to be introduced in the active region and the carriers from impurity atoms are totally localized in the active region such that

$$p + N_D^+ = n + N_A^- \quad (4)$$

where p and n are the hole and electron concentrations, respectively, in the active region and N_D and N_A are the donor and the acceptor concentrations, respectively. The distributions of the carriers and the dopants are assumed to be uniform in the active region. To simplify the calculation, we do not consider the effect of the band bending resulting from the nonuniform charge distribution. The hole concentration p includes those of the heavy holes, the light holes, and the spin-orbital split-off holes and the electron concentration n includes those of the Γ electrons and the X electrons.

The carrier-density-dependent bandgap shrinkage is an important effect in determining the emission wavelength. It has to be taken into account in gain spectrum calculation. We assume the gain spectrum is rigidly shifted by the shrinkage energy [15]

$$\Delta_{cv} = -1.6 \times 10^{-8}(p^{1/3} + n^{1/3})(\text{eV}) \quad (5)$$

where p and n are in units of cm^{-3}.

In our model, the total current is assumed to be composed of two components: the radiative recombination current and the leakage current. For 630-nm band GaInP–AlGaInP

lasers, leakage current is significant and usually dominates the other current component [10]. The nonradiative recombination current is neglected since the small split-off energy of the wide bandgap material suppresses the Auger recombination. Only the electron leakage current over the p-cladding layer is considered since it is much larger than the hole leakage current over the n-cladding layer. The detailed derivation of the formula for the leakage current can be found in [10] and the result is [16]

$$J_{\rm leakage} = \frac{1}{2}\left\{1+\sqrt{1+\left(\frac{2Z}{L_n}\right)^2} \cdot \coth\left[\frac{W_p}{2Z}\sqrt{1+\left(\frac{2Z}{L_n}\right)^2}\right]\right\}\frac{\mu_n}{\mu_p}\frac{n_{\rm clad}}{p_{\rm clad}}J_{\rm rad} \quad (6)$$

where $J_{\rm rad}$ is the radiative recombination current density and can be obtained from the recombination rate in the active region. μ_n and μ_p are the electron and the hole mobilities, $n_{\rm clad}$ and $p_{\rm clad}$ are the electron and the hole concentrations, L_n is the electron diffusion length in the p-cladding layer, W_p is the thickness of the p-cladding layer, Z is the effective field length defined as $Z = k_B T/qE$, where k_B is the Boltzmann constant, T is temperature, and E is the electric field in the p-cladding. The electric field E is related to the radiative recombination current by [10]

$$J_{\rm rad} \approx q\mu_p p_{\rm clad} E. \quad (7)$$

The carrier densities $p_{\rm clad}$ and $n_{\rm clad}$ are obtained by using the difference of quasi-Fermi levels at threshold obtained from the threshold condition (1) and requiring the charge neutrality in the cladding layer

$$p_{\rm clad} = n_{\rm clad} + N_{A,{\rm clad}} \quad (8)$$

where $N_{A,{\rm clad}}$ is the acceptor concentration in the p-cladding layer, $n_{\rm clad}$ includes the electrons in the Γ and the X valleys, and $p_{\rm clad}$ contains holes in the split-off bands as well as in the heavy-hole and the light-hole bands.

The material parameters of the AlGaInP system lattice-matched to GaAs are not as well known as those of the AlGaAs. In this work, they are taken mainly from the data reported recently by Meney *et al.* [17]. The Γ and X bandgaps of $(Al_xGa_{1-x})_{0.5}In_{0.5}P$ at 300 K are given by

$$E_g^{\Gamma} = 1.900 + 0.610x \quad \text{eV} \quad (9)$$

$$E_g^{X} = 2.204 + 0.085x \quad \text{eV} \quad (10)$$

The band discontinuities for unstrained $Ga_yIn_{1-y}P$ in $(Al_xGa_{1-x})_{0.5}In_{0.5}P$ barrier are assumed to be

$$-\Delta E_v = -0.5\Delta E_g(y) - 0.063x - 0.157x^2 \quad \text{eV} \quad (11)$$

$$\Delta E_c = 0.5\Delta E_g(y) + 0.574x - 0.157x^2 \quad \text{eV} \quad (12)$$

where $\Delta E_g(y)$ is the bandgap difference between $Ga_{0.5}In_{0.5}P$ and $Ga_yIn_{1-y}P$. The bandgap of $Ga_yIn_{1-y}P$ is given by fitting to those of InP, $Ga_{0.5}In_{0.5}P$, and GaP. The other parameters for $(Al_xGa_{1-x})_{0.5}In_{0.5}P$ used in the calculation are obtained by linear interpolation among those of InP, GaP, and AlP, which are listed in [10, Table I]. The refractive index for calculating optical modes is obtained from [18]. The mobilities of electrons and holes in the p-cladding layer are assumed to be $\mu_n = 100$ cm^2/Vs and $\mu_p = 10$ cm^2/Vs, respectively, and the electron diffusion length is $L_n = 0.6$ μm. In calculating the band structures of strained wells, we assume the deformation potentials $a_c : -a_v = 3{:}1$.

III. Results and Discussion

In this section, we show and discuss the calculation results for SCH lasers. The laser structures are composed of 8-nm $Ga_{0.6}In_{0.4}P$ tensile-strained QW's, 4-nm $(Al_{x_b}Ga_{1-x_b})_{0.5}In_{0.5}P$ barrier layers (sandwiched by the wells), two 100-nm $(Al_{x_b}Ga_{1-x_b})_{0.5}In_{0.5}P$ confining layers, and two 1-μm $(Al_{x_c}Ga_{1-x_c})_{0.5}In_{0.5}P$ cladding layers. The dopant concentration in the p-cladding layer is assumed to be 1×10^{18} cm^{-3} and that in the n-cladding layer is high sufficiently so that the hole leakage current can be neglected. The cavity length of the lasers is taken to be 500 μm and the internal loss α_i is assumed to be 10 cm^{-1}. The temperature is 300 K.

Fig. 3 shows the calculation results at threshold as functions of the dopant concentration in the active region for laser structures with three quantum wells ($N_w = 3$) and $(Al_{0.7}Ga_{0.3})_{0.5}In_{0.5}P$ cladding layers ($x_c = 0.7$). Three different Al contents of the barriers (or the confining layers) are considered, $x_b = 0.4$, 0.5, and 0.6. Fig. 3(a) shows the calculation results of the radiative recombination current density $J_{\rm rad}$. As can be seen, $J_{\rm rad}$ decreases with the increase in the donor concentration but increases with the increase in the acceptor concentration. This agrees with the theoretical results of Uomi [6] and can be explained by the asymmetry of the densities of states in the conduction and valence bands. It can be easily understood by using the simple relation $J_{\rm rad} \propto \Delta n_{\rm th}/\tau_s$. Here, τ_s is the spontaneous recombination lifetime. $\Delta n_{\rm th}$, the differential current density at threshold, is defined to be $\Delta n_{\rm th} = n_{\rm th} = n_0 = p_{\rm th} - p_0$. $n_{\rm th}$ and $p_{\rm th}$ are the densities of the electrons and the holes at threshold, respectively. n_0 and p_0 are those at thermal equilibrium. Introducing dopants to the active region causes reductions of both $\Delta n_{\rm th}$ and τ_s [6]. For n-type doping, due to the very low density of states in the conduction band, the reduction of $\Delta n_{\rm th}$ exceeds that of τ_s. This results in a decrease in $J_{\rm rad}$ compared with that of lasers with lower n-type doping concentration. On the other hand, the reduction of τ_s exceeds that of $\Delta n_{\rm th}$ when the active region is p-type doped, resulting in an increase in $J_{\rm rad}$. As can be seen in the figure, $J_{\rm rad}$ is significantly reduced by n-type doping in the active region (from 800–1100 to 500–600 A/cm^2). The lasers with $x_b = 0.4$ and 0.5 have higher $J_{\rm rad}$'s than the laser with $x_b = 0.6$, even though the optical confinement of the latter is poorer than the former. This is because the spontaneous recombination of the carriers which spills over the barriers is serious for lasers with low x_b values (low barrier height). In other words, the peak gain versus carrier-density curve is easier to saturate for lasers with shallower QW's [10]. The improvement in $J_{\rm rad}$ for the lasers with low x_b values by n-

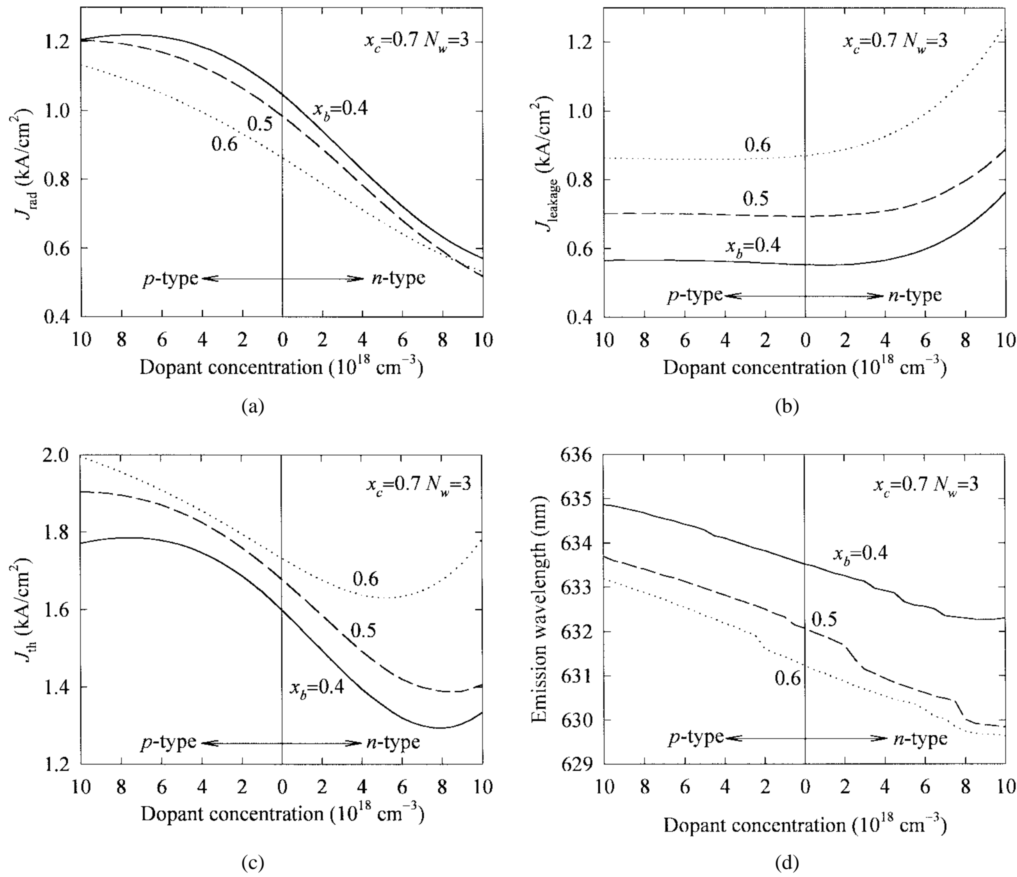

Fig. 3. (a) The radiative current density $J_{\rm rad}$, (b) the leakage current density $J_{\rm leakage}$, (c) the threshold current density $J{\rm th}$, and (d) the emission wavelength versus the dopant concentration in the active region of triple QW lasers $(Nw = 3)$ with $(Al_{0.7}Ga_{0.3})_{0.5}In_{0.5}P$ cladding layers $(x_c = 0.7)$. Three different Al contents of the confining layers are considered $(xb$ = 0.4, 0.5, and 0.6).

type doping is more significant. This is because the spill-over of holes is suppressed by n-type doping. In such lasers, the QW of the conduction band is much deeper than that of the valence band [see the band offsets (11) and (12)]. The holes are easier to spill over the barriers than the electrons. Introducing n-type doping suppresses the spill-over of holes more than enhances that of the electrons. One the other hand, introducing p-type doping does not only increase $\Delta n_{\rm th}/\tau_s$ but also enhances the spill-over of the holes, leading to the increase of $J_{\rm rad}$ with p-type doping.

Fig. 3(b) shows the calculation results of the leakage current $J_{\rm leakage}$. Although $J_{\rm rad}$ can be reduced significantly by n-type doping in the active region, $J_{\rm leakage}$ nevertheless increases with the n-type doping, as can be seen from the figure. The increase in $J_{\rm leakage}$ results from the increase of the quasi-Fermi level separation with the n-type doping. The quasi-Fermi level of the conduction band is much more sensitive to the electron density than that of the valence band to the hole density since the density of states in the conduction band is much lower than that in the valence band. Therefore, p-type doped lasers have a smaller quasi-Fermi level separation at threshold than n-type doped lasers. In addition, one can see that $J_{\rm leakage}$ does not depend on the p-type dopant concentration very much. $J_{\rm leakage}$ slightly increases with the p-type concentration although the quasi-Fermi level separation is reduced with the p-type doping. This is because the drift leakage current, which depends on the electric field in the p-cladding layer, is enhanced by the increase of $J_{\rm rad}$ [see (7)] when the active region is p-type-doped [10]. This increase of the drift leakage current compensates for the reduction of the diffusion leakage current which results from the reduction of the quasi-Fermi-level separation (and therefore the reduction of the electron density in the p-cladding layer). On the other hand, $J_{\rm leakage}$ is a strong function of the n-type dopant concentration since a significant increase of the diffusion leakage current is caused by the increase of the quasi-Fermi-level separation. One can also find that $J_{\rm leakage}$ is higher for lasers with a larger x_b. This is because the optical confinement is poorer for the lasers with a larger x_b. A poorer optical confinement means that it needs a higher gain or a higher carrier density to reach the threshold condition. So the quasi-Fermi-level separation is larger and $J_{\rm leakage}$ is higher for lasers with a larger x_b. It is noticed that the increase in $J_{\rm leakage}$ with the n-type dopant concentration is less than the reduction in $J_{\rm rad}$.

Fig. 3(c) shows the calculation results of the threshold current $J_{\rm th}$. The reduction in $J_{\rm th}$ by n-type doping is not as much as that in $J_{\rm rad}$ because of the increase in $J_{\rm leakage}$. However, the reduction of $J_{\rm th}$ is still significant for lasers with $x_b = $ 0.4 and 0.5. One can find that there is an optimum dopant concentration for a minimal $J_{\rm th}$ $(N_D \sim 8{\times}10^{18}$ cm$^{-3})$.

The emission wavelength can be significantly shortened by introducing the n-type doping, as shown in Fig. 3(d). The shift

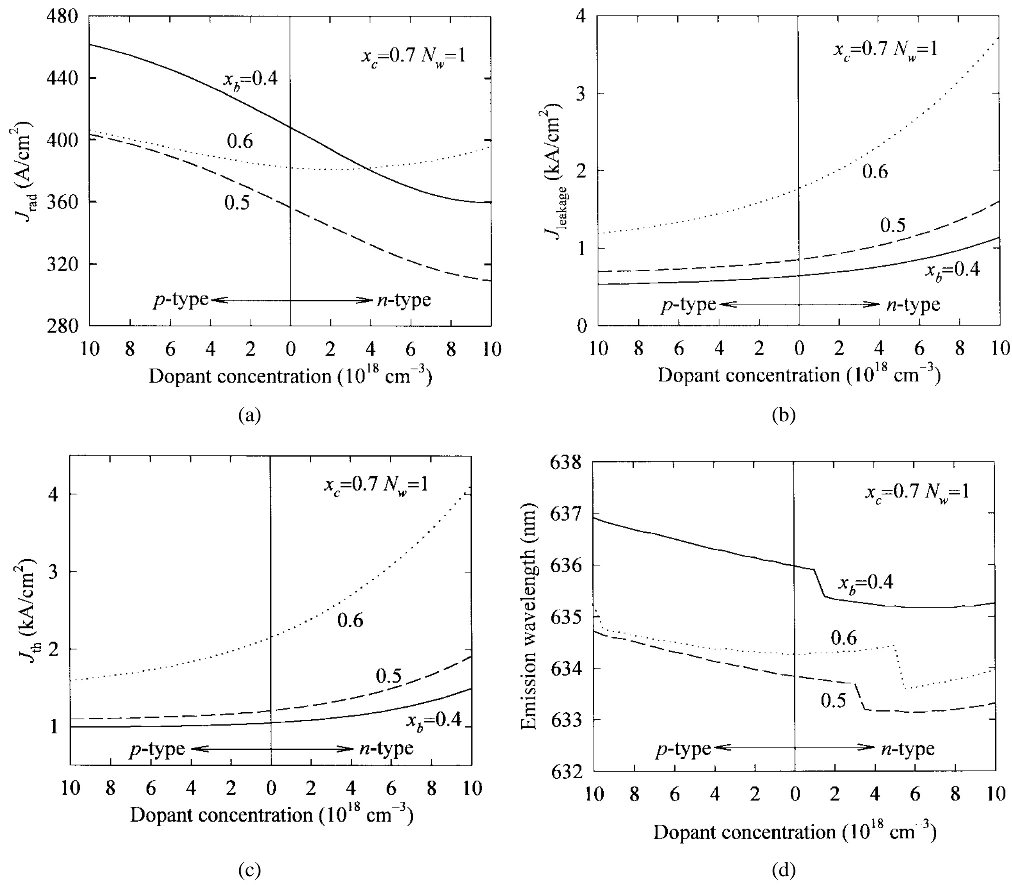

Fig. 4. (a) The radiative current density $J_{\rm rad}$, (b) the leakage current density $J_{\rm leakage}$, (c) the threshold current density $J{\rm th}$, and (d) the emission wavelength versus the dopant concentration in the active region of SQW lasers ($N_w = 1$) with $(Al_{0.7}Ga_{0.3})_{0.5}In_{0.5}P$ cladding layers ($x_c = 0.7$). Three different Al contents of the confining layers are considered (x_b = 0.4, 0.5, and 0.6).

of the wavelength is essentially due to the change of the quasi-Fermi-level separation at threshold. However, the effect of the carrier-density-dependent bandgap shrinkage also plays an important role in determining the amount of the wavelength shift [10]. The bandgap shrinkage suppresses the blue shift of the emission wavelength for n-type doping and enhances the red shift for p-type doping. As a result, the red shift of the emission wavelength for p-type doping is comparable to the blue shift for n-type doping although the quasi-Fermi-level separation at threshold is less sensitive to the p-type doping in the active region than the n-type doping.

The results described above are all for triple QW lasers. Fig. 3 shows the calculation results for laser structures with a single QW ($N_w = 1$) and $(Al_{0.7}Ga_{0.3})_{0.5}In_{0.5}P$ cladding layers ($x_c = 0.7$). The $J_{\rm rad}$'s, shown in Fig. 4(a), have values smaller than those for triple QW lasers in Fig. 3(a). This is because the active region is narrower for SQW lasers. A narrower active region means a higher gain is needed to reach the threshold condition. For the laser with $x_b = 0.6$, in addition to the narrow active region, the optical confinement is very poor so that a very high gain is needed at threshold. The spill-over of electrons may become important in this case and is enhanced significantly by n-type doping. The curve for $x_b = 0.6$ is therefore obviously different from the others.

The high threshold gain of the SQW lasers results in a large quasi-Fermi-level separation and hence a high leakage current. Fig. 4(b) shows the calculation results of $J_{\rm leakage}$. Different from the case of triple QW lasers, the amount of the increase in $J_{\rm leakage}$ with the n-type doping is more significant than the amount of reduction of $J_{\rm rad}$. This is because $J_{\rm leakage}$ is strongly sensitive to the variation of the quasi-Fermi-level separation as the n-type dopant concentration increases. $J_{\rm leakage}$ for the laser with $x_b = 0.6$ is unacceptably large. The threshold current density $J_{\rm th}$, shown in Fig. 4(c), is therefore not improved by n-type doping. Fig. 4(d) shows the calculation results of emission wavelength. Compared with the data for triple QW lasers [see Fig. 3 (d)], the wavelengths are longer. For larger quasi-Fermi separation, the wavelength should, however, be shorter. We attribute the result to the large amount of bandgap shrinkage for SQW lasers due to the high carrier density in the active region at threshold. This is also the reason why the emission wavelength for the laser with $x_b = 0.6$ is longer than that with $x_b = 0.5$ in our calculation result. From the figure, one can see the wavelength hopping at some critical n-type dopant concentration for each x_b. This phenomenon has been observed experimentally and is caused by the switching of the optical transition from lower energy levels to higher energy levels [7].

Although $J_{\rm th}$ can be reduced by n-type doping for triple QW lasers, the values of $J_{\rm th}$ are still too high. The reason is clearly that $J_{\rm leakage}$, which can not be reduced by n-type doping, plays an important part of the total current. Reducing

$J_{\rm leakage}$ is therefore a key issue for obtaining a 630-nm band GaInP–AlGaInP laser with low threshold current. There are several methods for reducing $J_{\rm leakage}$ [10]. Increasing the dopant concentration in the p-cladding layer can give a significant reduction in leakage current. In this case, the amount of minority carriers (the leakage carriers) becomes small and the electrical field is weak in the p-cladding layer [10]. However, it is not easy to obtain a heavily p-doped AlGaInP with high Al content. It has also been shown that increasing the Al content of the cladding layers can also reduce the leakage current efficiently. The bandgap of the cladding layers is widened in the case and the leakage carriers are significantly suppressed by the higher potential barrier. The cladding layers with higher Al content also give a tighter optical confinement. This, as has been mentioned above, can reduce the quasi-Fermi-level separation and further reduce the leakage current.

In the following, we show the calculation results for the laser structures containing $Al_{0.5}In_{0.5}P$ cladding layers ($x_c = 1$). Shown in Fig. 5 are the results for laser structures with three QW's ($N_w = 3$). As expected, the $J_{\rm rad}$, shown in Fig. 5(a), decreases with the n-type doping. We see that the $J_{\rm rad}$'s have an improvement of ~300 A/cm^2 compared to the results for the structures with $N_w = 3$ and $x_c = 0.7$ [see Fig. 3 (a)]. The improvement of $J_{\rm rad}$ is due to the tighter optical confinement. It needs a lower density of carriers (and therefore a lower carrier recombination rate) to reach threshold condition. The leakage current, as shown in Fig. 5(b), is also improved considerably compared to the data in Fig. 3(b) for the structures with $N_w = 3$ and $x_c = 0.7$. $J_{\rm leakage}$ can remain to be less than 400 A/cm^2. For $x_b = 0.6$, the improvement is more significant (from ~850 A/cm^2 for $x_c = 0.7$ to ~280 A/cm^2 for $x_c = 1$). Compared with $J_{\rm rad}, J_{\rm leakage}$ no longer plays a dominant part of the total current. This results in the decrease of $J_{\rm th}$ with the n-type doping, as shown in Fig. 5(c), similar to the case for $x_c = 0.7$. But the $J_{\rm th}$'s are much lower than those for $x_c = 0.7$. $J_{\rm th}$ of less than 700 A/cm^2 can be achieved for heavy n-type doping in the active region.

Fig. 6 shows the calculation results for laser structures with $N_w = 1$ and $x_c = 1$. Comparing the $J_{\rm rad}$'s shown in Fig. 6(a) with those in Fig. 4(a) for the case of $x_c = 0.7$, we find that the improvement of $J_{\rm rad}$ for $x_b = 0.4$ and 0.5 is slight, but for $x_b = 0.6$, because the spill-over of the carriers to continuum states is no longer important, the improvement is more significant. In addition, one can find that the curves for $x_b = 0.6$ in the two figures are obviously very different. Fig. 6(b) shows the results for $J_{\rm leakage}$. Similar to the other cases, $J_{\rm leakage}$ increases with n-type doping. However, the values of $J_{\rm leakage}$ are considerably lower than those for the case of $x_c = 0.7$. The threshold current, shown in Fig. 6(c), is therefore much lower. For $x_b = 0.4$ and 0.5, the minimal $J_{\rm th}$'s (~600 A/cm^2) occur when the active region is nearly undoped.

The calculation results for emission wavelength for the cases of $x_c = 1$ are essentially and quantitatively similar to those for the cases of $x_c = 0.7$. It is therefore not necessary to show the figures of emission wavelength for the cases of $x_c = 1$ here. Note that the n-type doping in the active region cannot give an advantage of reduction in threshold current for SQW lasers. But for triple QW lasers, because the leakage current is not so important as for SQW lasers, the threshold current can be reduced and the emission wavelength can be shortened by n-type doping.

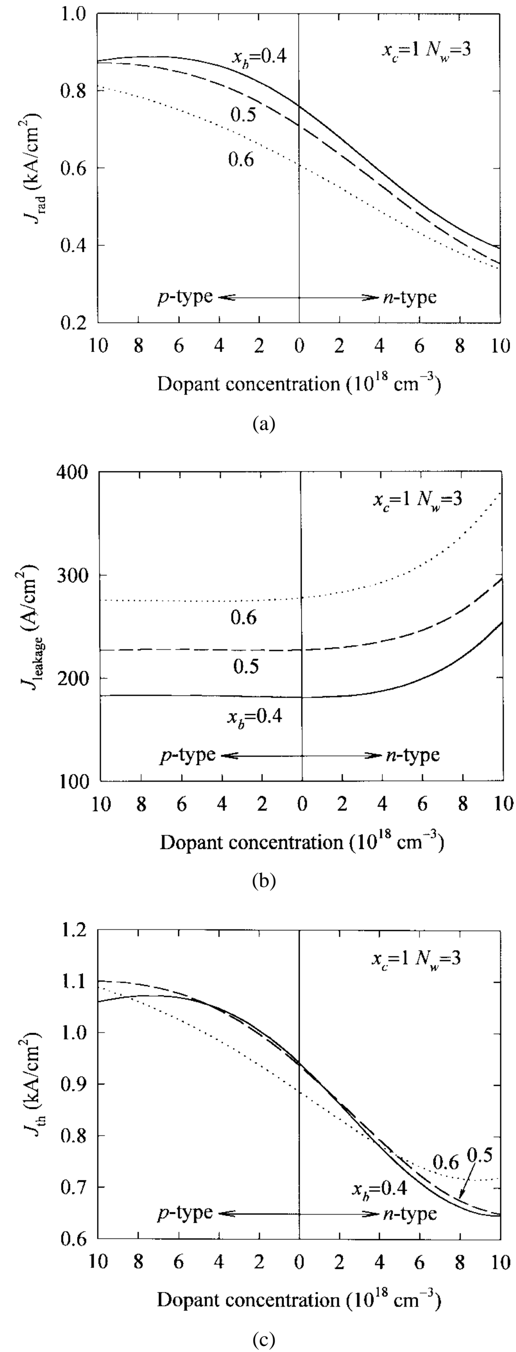

Fig. 5. (a) The radiative current density $J_{\rm rad}$, (b) the leakage current density $J_{\rm leakage}$, and (c) the threshold current density $J_{\rm th}$ versus the dopant concentration in the active region of triple QW lasers ($N_w = 3$) with $Al_{0.5}In_{0.5}P$ cladding layers ($x_c = 1$). Three different Al contents of the confining layers are considered ($x_b = 0.4$, 0.5, and 0.6).

In the calculation, we assume the dopants are uniformly distributed in the active region and do not consider the effect of the nonuniform distribution of charges. In practice, the carriers lie in the active region nonuniformly. This results in

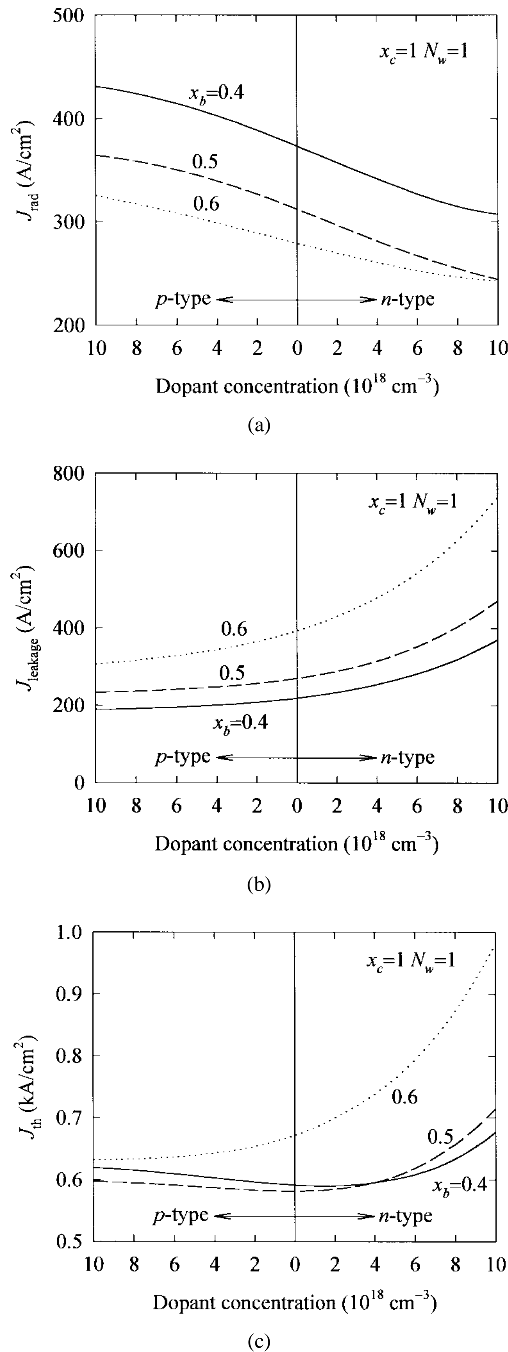

Fig. 6. (a) The radiative current density $J_{\rm rad}$, (b) the leakage current density $J_{\rm leakage}$, and (c) the threshold current density $J_{\rm th}$ versus the dopant concentration in the active region of SQW lasers ($N_w = 1$) with $Al_{0.5}In_{0.5}P$ cladding layers ($x_c = 1$). Three different Al contents of the confining layers are considered (x_b = 0.4, 0.5, and 0.6).

band bending and modification of the band structures, both of which further influence the carrier distribution. One has to solve simultaneously the equation governing the carrier distribution (the effective-mass equation) and that governing the band bending (the Poisson equation) self-consistently to obtain more reasonable results. The uniform doping in the active region gives rise to an additional problem. We have found from Figs. 3(c) and 5(c) that the threshold current can be reduced considerably by heavy n-type doping in the active region ($N_D \sim 8\times10^{18}$ cm^{-3}). This high dopant concentration in the active region may result in increases of the optical loss. This disadvantage has been overcome by using δ-doping or modulation doping near the active region. It is also necessary to consider the band-bending effect in theoretical calculation for the nonuniformly doping. However, considering the effect of band bending will greatly increase the complication of computation. Although we do not consider this effect, the calculation results in this work should be essentially similar to those with the band-bending effect taken into account.

IV. Conclusion

We have theoretically analyzed 630-nm-band GaInP–AlGaInP tensile-strained QW lasers with a doped active region. The results show that the threshold current can be reduced and the emission wavelength can be shortened by introducing n-type doping to multiquantum (triple)-well lasers. But for SQW lasers, the threshold current increases with the n-type doping because of the large increase in the leakage current.

References

[1] A. Valster, C. J. Van Der Poel, M. N. Finke, and M. J. B. Boermans, "Effect of strain on the threshold current of GaInP/AlGaInP quantum well lasers emitting at 633 nm," in *Tech. Dig., 13th IEEE Int. Semiconductor Laser Conf.*, Takamatsu, Japan, 1992, paper G1.

[2] P. Blood and P. M. Smowton, "Strain dependence of threshold current in fixed-wavelength GaInP laser diodes," *IEEE J. Select. Topics Quantum Electron.*, vol. 1, pp. 707–711, 1995.

[3] D. Ahn, S. J. Yoon, S. L. Chuang, and C. S. Chang, "Theory of optical gain in strained-layer quantum wells within the 6 × 6 Luttinger–Kohn model," *J. Appl. Phys.*, vol. 78, pp. 2489–2497, 1995.

[4] S. Kamiyama, M. Monnoh, K. Ohnaka, and T. Uenoyama, "Studies of threshold current dependence on compressive and tensile strain of 630 nm GaInP/AlGaInP multi-quantum-well lasers," *J. Appl. Phys.*, vol. 75, pp. 8201–8203, 1994.

[5] S. Kamiyama, T. Uenoyama, M. Monnoh, and K. Ohnaka, "Theoretical studies of GaInP-AlGaInP strained quantum-well lasers including spin-orbit split-off band effect," *IEEE J. Quantum Electron.*, vol. 31, pp. 1409–1417, 1995.

[6] K. Uomi, "Modulation-doped multi-quantum well (MD-MQW) lasers: I. Theory," *Jpn. J. Appl. Phys.*, vol. 29, pp. 81–87, 1990.

[7] S. M. Shank, J. A. Varriano, and G. W. Wicks, "Single quantum well GaAs/AlGaAs separate confinement heterostructure lasers with n-type modulation doped cores," *Appl. Phys. Lett.*, vol. 61, pp. 2851–2853, 1992.

[8] T. Yamamoto, T. Watanabe, S. Ide, K. Tanaka, H. Nobuhara, and K. Wakao, "Low threshold current density 1.3-μm strained-layer quantum-well lasers using n-type modulation doping," *IEEE Photon. Technol. Lett.*, vol. 6, pp. 1165–1166, 1994.

[9] O. Buchinsky, M. Blumin, R. Sarfaty, D. Fekete, I. Samid, and M. Yust, "n-type delta-doped quantum well lasers with extremely low transparency current density," *Appl. Phys. Lett.*, vol. 68, pp. 2043-2045, 1996.

[10] S. T. Yen and C. P. Lee, "Theoretical analysis of 630-nm band GaInP/AlGaInP strained quantum well lasers considering continuum states," *IEEE Quantum Electron.*, vol. 33, pp. 443–456, 1996.

[11] C. S. Chang and S. L. Chuang, "Modeling of strained quantum-well lasers with spin-orbital coupling," *IEEE J. Select. Topics Quantum Electron.*, vol. 1, pp. 218–229, 1995.

[12] Z. Ikonic, V. Milanovic, and D. Tjakin, "Bound-free intraband absorption in GaAs-Al_xGa_{1-x}As semiconductor quantum wells," *Appl. Phys. Lett.*, vol. 54, pp. 247–249, 1989.

[13] T. Ohtoshi and M. Yamanishi, "Optical line shape functions in quantum-well and quantum-wire structures," *IEEE Quantum Electron.*, vol. 27, pp. 46–53, 1991.

[14] M. Asada, "Intraband relaxation effect on optical spectra," in *Quantum Well Lasers*, P. S. Zory, Jr., Ed. San Diego, CA: Academic, 1993, pp. 97–130.

[15] F. Stern, "Calculated spectral dependence of gain in excited GaAs," *J. Appl. Phys.*, vol. 47, pp. 5382–5386, 1976.

[16] S. R. Chinn, P. S. Zory, and A. R. Reisinger, "A model for GRIN-SCH-SQW diode lasers," *IEEE J. Quantum Electron.*, vol. 24, pp. 2191–2214, 1988.

[17] A. T. Meney, A. D. Prins, A. F. Phillips, J. L. Sly, E. P. O'Reilly, D. J. Dunstan, A. R. Adams, and A. Valster, "Determination of the band structure of disordered AlGaInP and its influence on visible-laser characteristics," *IEEE J. Select. Topics Quantum Electron.*, vol. 1, pp. 697–706, 1995.

[18] D. Bour, "AlGaInP quantum well lasers," in *Quantum Well Lasers*, P. S. Zory, Jr., Ed. San Diego, CA: Academic, 1993, pp. 415–460.

Shun Tung Yen, photograph and biography not available at the time of publication.

Chien-Ping Lee (M'80–SM'94), photograph and biography not available at the time of publication.